Electroweak physics at the LHC

J Berryhill[1] and A Oh[2]

[1] Fermi National Accelerator Laboratory, Batavia, IL, USA

[2] School of Physics and Astronomy, University of Manchester, Manchester, UK

Abstract. The Large Hadron Collider (LHC) has completed in 2012 its first running phase and the experiments have collected data sets of pp collisions at center-of-mass energies of 7 and 8 TeV with an integrated luminosity of about 5 $fb^{-1}$and 20 fb^{-1}, respectively. Analyses of these data sets have produced a rich set of results in the electroweak sector of the standard model. This article reviews the status of electroweak measurements of the ATLAS and CMS experiments at the LHC and discusses phenomenological developments in the electroweak sector.

PACS numbers: 12.15.-y, 12.60.Cn, 14.70.-e

Submitted to: *J. Phys. G: Nucl. Part. Phys.*

At a hadron collider, the most fundamental tests of electroweak boson couplings to fermions are measurements of the kinematic properties of Drell-Yan (DY) lepton pair production. At leading order, Drell-Yan production occurs when a quark–anti-quark pair in the intial state annihilates into an electroweak boson, which subsequently decays to a lepton pair. Differential cross section calculations exist for next-to-next-to leading order (NNLO) QCD corrections as well as NLO electroweak corrections. In the EFT context, such a process is sensitive to four-fermion contact interactions of the type

$$\begin{aligned}\mathcal{L} = \tfrac{g^2}{\Lambda^2}\,[\quad & \eta_{\rm LL}\ (\overline{q}_{\rm L}\gamma_\mu q_{\rm L})\,(\overline{\ell}_{\rm L}\gamma^\mu \ell_{\rm L}) \\ & +\eta_{\rm RR}\,(\overline{q}_{\rm R}\gamma_\mu q_{\rm R})\,(\overline{\ell}_{\rm R}\gamma^\mu \ell_{\rm R}) \\ & +\eta_{\rm LR}\,(\overline{q}_{\rm L}\gamma_\mu q_{\rm L})\,(\overline{\ell}_{\rm R}\gamma^\mu \ell_{\rm R}) \\ & +\eta_{\rm RL}\,(\overline{q}_{\rm R}\gamma_\mu q_{\rm R})\,(\overline{\ell}_{\rm L}\gamma^\mu \ell_{\rm L})\ ]\,,\end{aligned} \tag{1}$$

where g is a coupling constant, Λ is the contact interaction scale, and $q_{\rm L,R}$ and $\ell_{\rm L,R}$ are left-handed and right-handed quark and lepton fields, respectively. The parameters $\eta_{i,j}$ denote the relative interference of the operators; the experiments have considered the cases $\eta_{\rm LR} = \eta_{\rm RL} = \pm 1$, $\eta_{\rm LL} = \pm 1$, or $\eta_{\rm RR} = \pm 1$.

Experiments select electron or muon pairs above trigger thresholds: CMS selects leading lepton $p_T > 17$ GeV and second leading lepton $p_T > 8$ GeV inclusively, and ATLAS selects high mass events with both lepton $p_T > 25$ GeV. Backgrounds to Drell-Yan production are relatively small, and consist of real prompt lepton pair production from top quark or boson pairs, as well as fake electrons from QCD jets. The real lepton pair background is flavor democratic, and can therefore be reliably estimated from $e\mu$ pair production. Fake electron production is typically estimated from background enriched QCD jet samples, from which the fake electron rate can be measured, convolved with electron-jet control samples.

Figure 1 shows the Drell-Yan cross section at high electron pair mass measured by ATLAS at 7 TeV [1]. The cross section uncertainty is predominantly systematic below 400 GeV in pair mass and predominantly statistical above 400 GeV. The data are compared with an NNLO QCD prediction with NLO electroweak corrections, provided by the FEWZ 3.1 generator [**?**]. The prediction also includes photon induced lepton pair production, which generally increases cross section estimates by a few percent. The FEWZ prediction generally underestimates the cross section, however a correlated chi-squared analysis concludes that this is not statistically significant.

Figure 2 shows the Drell-Yan cross section for electron or muon pairs measured by CMS at 8 TeV [6]. Agreement with the FEWZ prediction is observed over the entire measured mass range, from 15 GeV to 2000 GeV. CMS has also measured the double differential cross section with respect to dilepton rapidity in several bins of dilepton mass, as well as a differential cross section ratio between the 8 TeV and 7 TeV data, which has small experimental and theoretical uncertainties.

In the absence of observed disagreements with predictions at the highest dilepton masses, the data are analyzed to constrain the size of anomalous contact interactions. Assuming a fixed, strong value for the coupling ($g^2/4\pi = 1$), limits can be obtained

on the contact interaction scale Λ. ATLAS estimates a lower limit of 17 to 26 TeV on Λ, where the strongest lower limits correspond to constructive interference scenarios (especially LR+RL), and the weakest to destructive interference scenarios [10]. CMS has limits with similar sensitivity estimated for LL contact interactions [9].

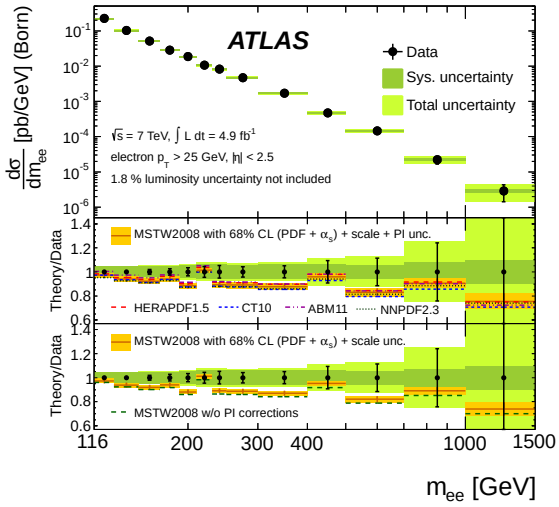

Figure 1. Measured differential cross-section at the Born level within the fiducial region (electron $p_{\mathrm{T}} > 25$ GeV and $|\eta| < 2.5$) with statistical, systematic, and combined statistical and systematic (total) uncertainties, excluding the 1.8% uncertainty on the luminosity. On the left, in the upper ratio plot, the photon-induced (PI) corrections have been added to the predictions obtained from the MSTW2008, HERAPDF1.5, CT10, ABM11 and NNPDF2.3 NNLO PDFs, and for the MSTW2008 prediction the total uncertainty band arising from the PDF, α_s, renormalisation and factorisation scale, and photon-induced uncertainties is drawn. The lower ratio plot shows the influence of the photon-induced corrections on the MSTW2008 prediction, the uncertainty band including only the PDF, α_s and scale uncertainties.

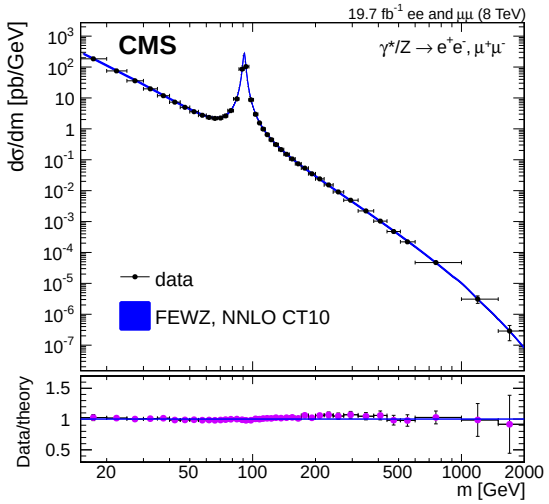

Figure 2. The DY differential cross section as measured in the combined dilepton channel and as predicted by NNLO FEWZ 3.1 with CT10 PDF calculations, for the full phase space.

3.2. Inclusive di-boson production

ATLAS $W^{\pm}\gamma$ $Z\gamma$ 7 TeV [11]
CMS $W^{\pm}\gamma/Z\gamma$ 7 TeV [12]
CMS $Z(\nu\bar{\nu})\gamma$ 7 TeV [13]
CMS $Z\gamma$ 8 TeV [14]
ATLAS simultaneous tt/WW/Z cross section 7 TeV [15]
ATLAS WW 7 TeV [16]
ATLAS WW+WZ cross section 7 TeV [17]
ATLAS WW 8 TeV [18]
CMS WW2l2n 7 TeV [19]
CMS WWlnjj 7 TeV [20]
CMS WW/ZZ 8 TeV [21]
CMS WW2l2n 8 TeV(CMS-PAS-SMP-14-016, to be published)
ATLAS WZ 7 TeV [22]
CMS VZ 8 TeV [23]
CMS WZ at 7+8 TeV(CMS-PAS-SMP-12-006, to be published)

3.2.1. ZZ production

The production of ZZ in proton-proton collisions has been one of the first di-boson processes measured at the LHC. The SM process is and an important and irreducible background to resonance searches and Higgs production. The production at leading order is dominated by quark anti-quark annihilation in the t and u-channel, whereas the s-channel process is forbidden in the SM (see also Figure 3). The gluon fusion process contributes about 6% to the total production cross section.

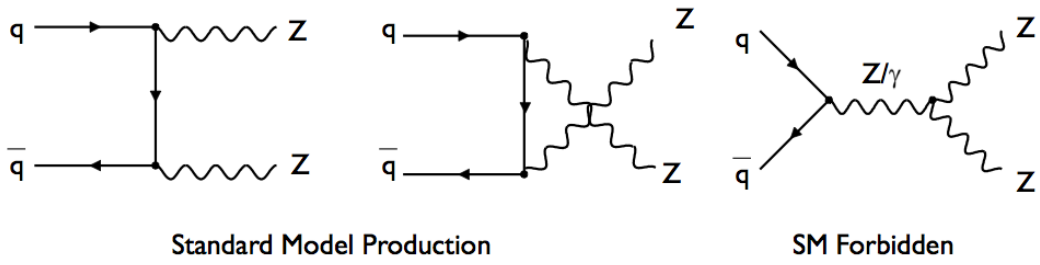

Figure 3. Leading order Feynman diagrams of ZZ production in the dominant $q\bar{q}$ channel. The ZZ production via the s-channel is not allowed in the SM.

Precision measurements use the leptonic decay modes of the Z to reduce the impact of QCD backgrounds. The four lepton final state provides an almost background free signature, at the expense of a relatively small branching ratio $BR(ZZ) \to \ell^+\ell^-\ell^+\ell^- = 0.101^2 \cdot \frac{4}{9} = 0.0045$ [**?**]. The di-lepton and missing energy channel can exploit the one order of magnitude higher branching ratio of $BR(ZZ \to \ell^+\ell^-\nu\bar{\nu}) = 0.101 \cdot 0.20 \cdot 2 \cdot \frac{2}{3} = 0.0269$, at the expense of high background levels.

The ATLAS collaboration has published results on the 7 TeV data-set in the $\ell^+\ell^-\ell^+\ell^-$ and $\ell^+\ell^-\nu\bar{\nu}$ final state [24]. The CMS collaboration has analysed the full 7 and 8 TeV data sets in both the $\ell^+\ell^-\ell^+\ell^-$ [25, 26] and $\ell^+\ell^-\nu\bar{\nu}$ final state [27].

Theoretical predictions for ZZ production are available at NLO in α_s [**?**]. In addition, electroweak corrections at NLO have been calculated [**?**, **?**].

The event selection for the $\ell^+\ell^-\ell^+\ell^-$ final state requires exactly four leptons fulfilling a set of cuts on kinematic quantities. ATLAS and CMS use similar criteria as listed in detail in Table **??**. While ATLAS uses $l = e, \mu$, CMS includes also $Z \to \tau^+\tau^-$ with subsequent hadronic and leptonic τ decays. ATLAS uses in addition forward leptons outside the ID tracker to increase the acceptance by 6% for electrons and 10% for muons. The $\ell^+\ell^-\ell^+\ell^-$ channels offers the cleanest event sample with a background level of only $2-3\%$ from $Z + jets$, , and di-boson events. The background is estimated from data by control regions with looser selection criteria.

Events in the $\ell^+\ell^-\nu\bar{\nu}$ final state are characterized by exactly two leptons and missing energy. The event selection requires a leptonic Z candidate and missing energy in the event. Both experiments used refined observables of missing energy with additional information to improve the rejection against instrumental background. The background level is in the same order as the signal and substantially higher then for $\ell^+\ell^-\ell^+\ell^-$. Main background sources are $V + jets$, and di-boson production. ATLAS and CMS

use data driven techniques to constrain the dominant background sources.

Besides the total cross section for the $pp \rightarrow ZZ$ production process, both experiments measure also fiducial and differential cross sections. The results are summarized in Tabel 2. ATLAS and CMS use different definitions of the fiducial phase space which needs to be taken into account to make a direct comparison is possible. For the total cross section a slightly different mass range for the Z mass range is used, where CMS uses a wider range of 60 GeV $< m_Z <$ 120 GeV then ATLAS with 76 GeV $< m_Z <$ 116 GeV, which contributes to the difference in the quoted predicted cross section. Agreement of experimental and theoretical cross section values is observed.

Table 1. default

Experiment	decay channel	$\sqrt{s}$	measured σ_{total} [pb]	predicted σ_{total}
ATLAS	$\ell^+\ell^-\ell^+\ell^-$, $\ell^+\ell^-\nu\bar{\nu}$	7 TeV	6.7 $\pm$ 0.7 (stat.) $^{+0.4}_{-0.3}$ (syst.) $\pm$ 0.3 (lumi.)	$6.18^{+0.25}_{-0.18}$
CMS	$\ell^+\ell^-\ell^+\ell^-$	7 TeV	6.2 $\pm$ $^{+0.9}_{-0.8}$ (stat.) $^{+0.4}_{-0.3}$ (syst.) $\pm$ 0.1 (lumi.)	6.3$\pm$0.4
CMS	$\ell^+\ell^-\nu\bar{\nu}$	7 TeV	5.2 $\pm$ $^{+1.5}_{-1.4}$ (stat.) $^{+1.4}_{-1.1}$ (syst.) $\pm$ 0.2 (lumi.)	6.1$\pm$0.3
CMS	$\ell^+\ell^-\ell^+\ell^-$	8 TeV	7.7 $\pm$ 0.5 (stat.) $^{+0.5}_{-0.4}$ (syst.) $\pm$ 0.2 (lumi.)	7.7$\pm$0.6
CMS	$\ell^+\ell^-\nu\bar{\nu}$	8 TeV	6.9 $\pm$ 0.8 (stat.) $^{+1.8}_{-1.4}$ (syst.) $\pm$ 0.3 (lumi.)	7.6$\pm$0.3

Table 2. Summary of measured ZZ production cross sections from ATLAS and CMS at 7 and 8 TeV centre-of-mass energies in the four lepton and $\ell^+\ell^-\nu\bar{\nu}$ final state.

Limits on ATGC parameters are determined with differential distributions of the invariant di-boson mass (CMS, four lepton channel), the transverse momentum of the leading lepton (CMS, $\ell^+\ell^-\nu\bar{\nu}$-channel), or the transverse momentum of the leading Z(ATLAS, all channels). A comparison of the measured and predicted differential cross sections in the four-lepton invariant mass is shown from CMS in Figure 4. Also shown is the prediction in the presence of a non-zero value of the anomalous coupling parameter $f_4^Z = 0.015$, which shows an enhancement over the SM value at high invariant masses.

Both experiment publish 95% CL limits on aTGC without form factors in the $\ell^+\ell^-\ell^+\ell^-$ and $\ell^+\ell^-\nu\bar{\nu}$ channels. The results are summarized in Figure **??**.

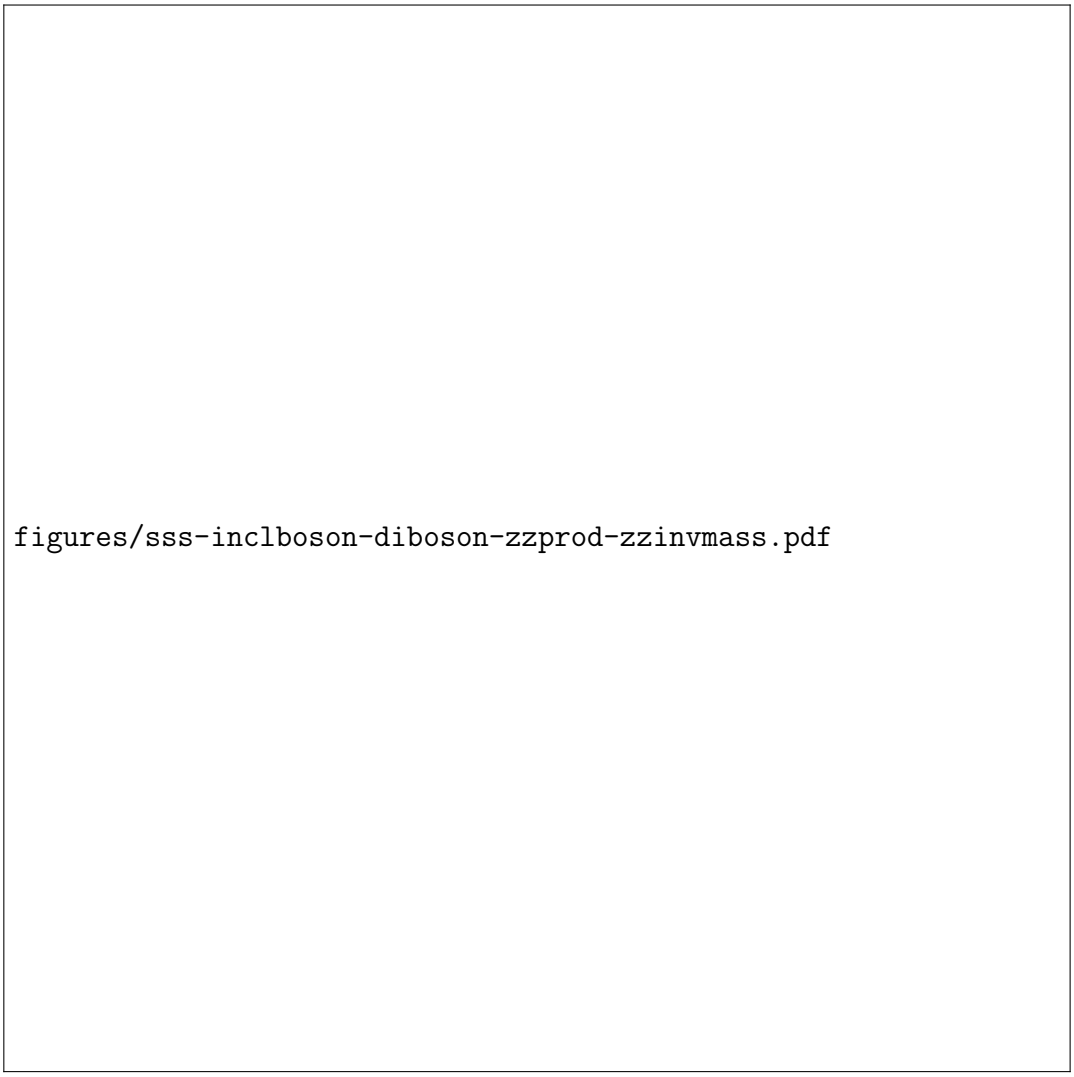

Figure 4. Distribution of the four-lepton reconstructed mass for the combined $4e$, 4μ, and $2e2\mu$ channels from CMS [26]. Points represent the data, the shaded histogram labeled ZZ represents the predictions for ZZ signal, the histograms labeled $W^{\pm}Z/Z$+jets shows background estimated form data. The dashed and dotted histograms indicate the SM expectation (f4Z = 0) and in the presence of an ATGC (f4Z = 0.015) with all the other anomalous couplings set to zero. The last bin includes all entries with masses above 1000 GeV.

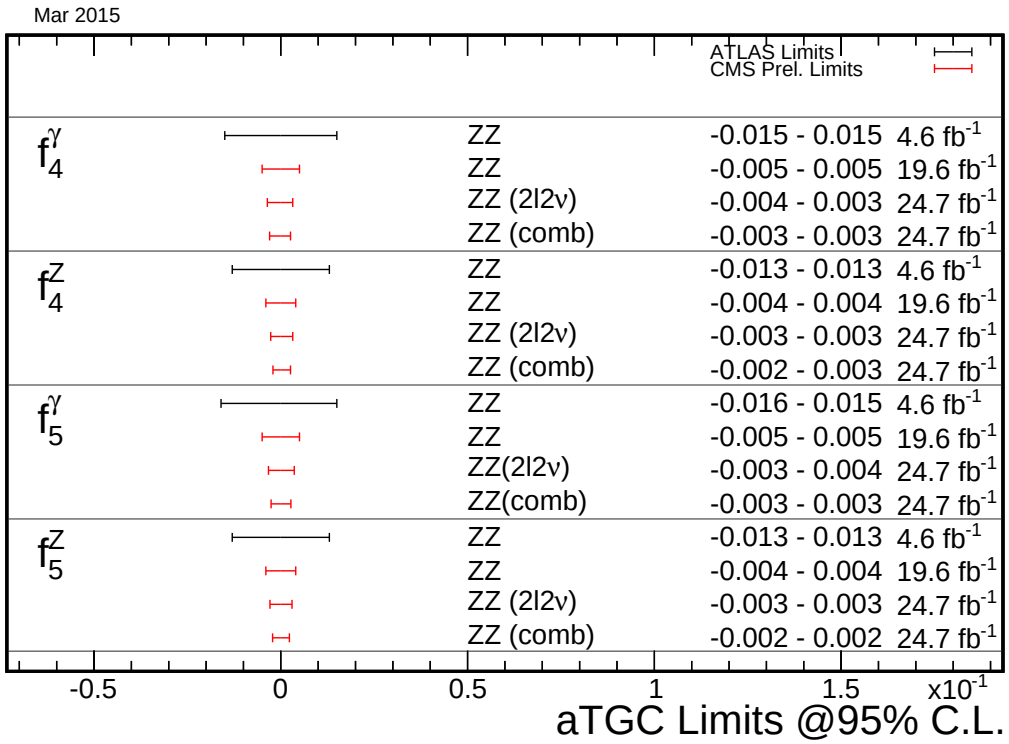

Figure 5. Comparison of the limits on $f_{40}^V$and $f_{50}^V$from ATLAS and CMS in the $\ell^+\ell^-\ell^+\ell^-$ and $\ell^+\ell^-\nu\bar{\nu}$ channel at 7 and 8 TeV.

3.3. Inclusive tri-boson production

ATLAS $W\gamma\gamma$ [28]
CMS WVgamma 8 TeV [29]

4. Exclusive boson production

4.1. Exclusive single boson production, vector-boson fusion

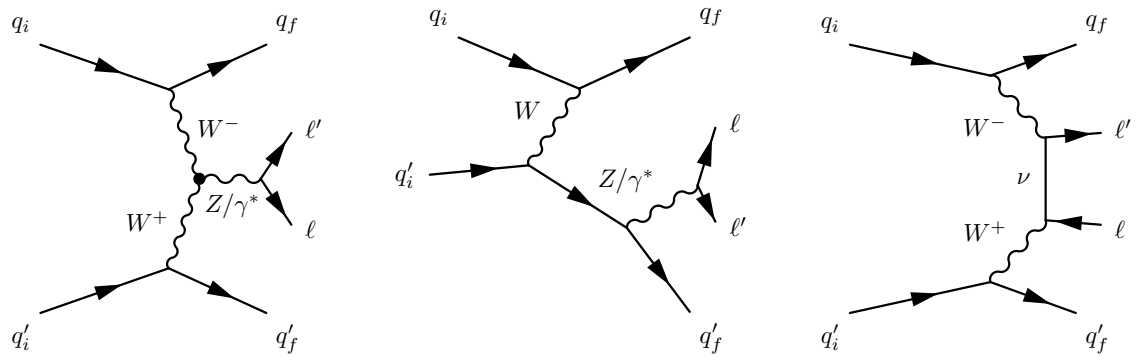

Figure 6. Representative Feynman diagrams for dilepton production in association with two jets from purely electroweak contributions: (left) vector boson fusion, (middle) bremsstrahlung-like, and (right) multiperipheral production.

ATLAS VBF Z 7 TeV [30]
CMS VBF Z 7 TeV [31]
CMS VBF Z 8 TeV [32] Figure 7

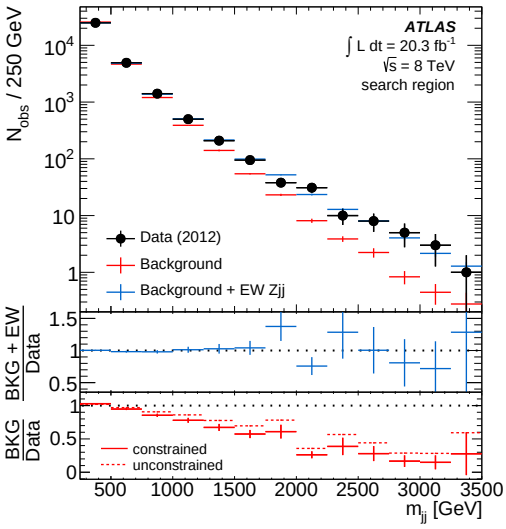
ATLAS
∫ L dt = 20.3 fb-1
√s = 8 TeV
search region
N_obs / 250 GeV
Data (2012)
Background
Background + EW Zjj
BKG + EW / Data
BKG / Data
constrained
unconstrained
m_jj [GeV]

Figure 7.

4.2. Exclusive di-boson production, vector-boson scattering

CMS WWexcl 7 TeV [34] ATLAS SSWW 8 TeV [33] CMS SSWW 8 TeV [35]

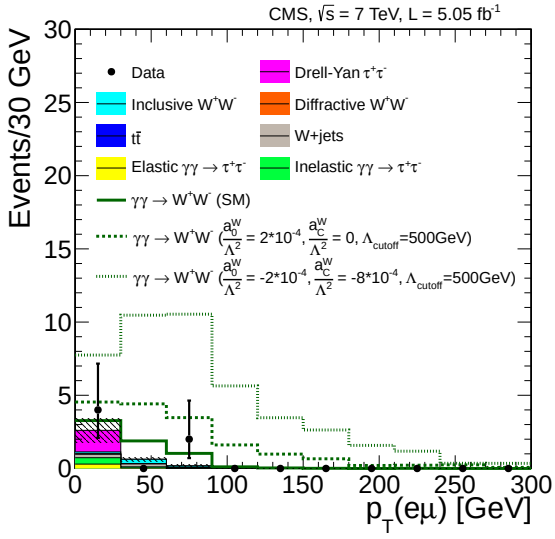
CMS, √s = 7 TeV, L = 5.05 fb-1
Events/30 GeV
Data
Drell-Yan τ+τ-
Inclusive W+W-
Diffractive W+W-
tt̄
W+jets
Elastic γγ → τ+τ-
Inelastic γγ → τ+τ-
γγ → W+W- (SM)
γγ → W+W- (a0W/Λ2 = 2*10-4, acW/Λ2 = 0, Λcutoff=500GeV)
γγ → W+W- (a0W/Λ2 = -2*10-4, acW/Λ2 = -8*10-4, Λcutoff=500GeV)
pT(eμ) [GeV]

Figure 8.

5. Electroweak (precision) tests of the standard model

5.1. Test of tri-boson vertex

ATLAS Wgamma Zgamma 7 TeV [11]
ATLAS WW 7 TeV [16]
ATLAS WW+WZ cross section 7 TeV [17]
ATLAS WZ 7 TeV [22]
ATLAS ZZ4l,ZZ2l2v 7 TeV [24]
CMS ZZ4l 8 TeV [26]
CMS ZZ4l 7 TeV [25]
CMS WW2l2n 7 TeV [19]
CMS WWlnjj 7 TeV [20]
CMS WW2l2n 8 TeV(CMS-PAS-SMP-14-016, to be published)
CMS $W^{\pm}\gamma/Z\gamma$ 7 TeV [12]
CMS Znngamma 7 TeV [13]
CMS $Z\gamma$ 8 TeV [14]
CMS $ZZ \to \ell^{\pm}\ell^{-}\nu\bar{\nu}$ 7+8 TeV [27]

5.2. Test of tetra-boson vertex

ATLAS $W\gamma\gamma$ 8 TeV [28]
ATLAS SSWW 8 TeV [33]
CMS WVgamma 8 TeV [29]
CMS WWexcl 7 TeV [34]
CMS SSWW 8 TeV [35]

5.3. Z AFB and sin thetaW

ATLAS weak mixing angle [36]
CMS weak mixing angle [37]
CMS Drell–Yan AFB 7 TeV [38]
CMS Drell–Yan AFB 8 TeV, g_1^Z, κ^Z, λ^Z(CMS-PAS-SMP-14-004, to be published)

5.4. W mass

6. Summary

ATLAS [39] CDF [40] CMS [41] D0 [42] LHCb [43]

CDF Z asymmetry muon [44] CDF Z asymmetry electron [45] CDF W mass PRD [46] CDF W mass PRL [47]

D0 W asymmetry electron [48] D0 W asymmetry muon [49] D0 W mass PRD [50] D0 W mass PRL [51]

CDF+D0 W mass combination [52]

Snowmass electroweak [53]
Wmass PDF [54]

Acknowledgments

Acknowledgments go here.

[1] Aad G *et al.* (ATLAS Collaboration) 2013 *Phys.Lett.* **B725** 223–242 (*Preprint* 1305.4192)
[2] Aad G *et al.* (ATLAS Collaboration) 2014 *JHEP* **1406** 112 (*Preprint* 1404.1212)
[3] Aad G *et al.* (ATLAS Collaboration) 2014 (*Preprint* 1406.3660)
[4] Aad G *et al.* (ATLAS Collaboration) 2013 *Phys.Lett.* **B720** 32–51 (*Preprint* 1211.6899)
[5] Chatrchyan S *et al.* (CMS Collaboration) 2013 *JHEP* **1312** 030 (*Preprint* 1310.7291)
[6] Khachatryan V *et al.* (CMS Collaboration) 2015 *Eur.Phys.J.* **C75** 147 (*Preprint* 1412.1115)
[7] Khachatryan V *et al.* (CMS Collaboration) 2015 (*Preprint* 1504.03512)
[8] Khachatryan V *et al.* (CMS Collaboration) 2015 (*Preprint* 1504.03511)
[9] Khachatryan V *et al.* (CMS) 2015 *JHEP* **1504** 025 (*Preprint* 1412.6302)
[10] Aad G *et al.* (ATLAS) 2014 *Eur.Phys.J.* **C74** 3134 (*Preprint* 1407.2410)
[11] Aad G *et al.* (ATLAS Collaboration) 2013 *Phys.Rev.* **D87** 112003 (*Preprint* 1302.1283)
[12] Chatrchyan S *et al.* (CMS Collaboration) 2014 *Phys.Rev.* **D89** 092005 (*Preprint* 1308.6832)
[13] Chatrchyan S *et al.* (CMS Collaboration) 2013 *JHEP* **1310** 164 (*Preprint* 1309.1117)
[14] Khachatryan V *et al.* (CMS Collaboration) 2015 *JHEP* **1504** 164 (*Preprint* 1502.05664)
[15] Aad G *et al.* (ATLAS Collaboration) 2015 *Phys.Rev.* **D91** 052005 (*Preprint* 1407.0573)
[16] Aad G *et al.* (ATLAS Collaboration) 2013 *Phys.Rev.* **D87** 112001 (*Preprint* 1210.2979)
[17] Aad G *et al.* (ATLAS Collaboration) 2015 *JHEP* **1501** 049 (*Preprint* 1410.7238)
[18] 2014 Measurement of the W^+W^- production cross section in proton-proton collisions at $\sqrt{s} = 8$ TeV with the ATLAS detector Tech. Rep. ATLAS-CONF-2014-033 CERN Geneva
[19] Chatrchyan S *et al.* (CMS Collaboration) 2013 *Eur.Phys.J.* **C73** 2610 (*Preprint* 1306.1126)
[20] Chatrchyan S *et al.* (CMS Collaboration) 2013 *Eur.Phys.J.* **C73** 2283 (*Preprint* 1210.7544)
[21] Chatrchyan S *et al.* (CMS Collaboration) 2013 *Phys.Lett.* **B721** 190–211 (*Preprint* 1301.4698)
[22] Aad G *et al.* (ATLAS Collaboration) 2012 *Eur.Phys.J.* **C72** 2173 (*Preprint* 1208.1390)
[23] Chatrchyan S *et al.* (CMS Collaboration) 2014 *Eur.Phys.J.* **C74** 2973 (*Preprint* 1403.3047)
[24] Aad G *et al.* (ATLAS Collaboration) 2013 *JHEP* **1303** 128 (*Preprint* 1211.6096)
[25] Chatrchyan S *et al.* (CMS Collaboration) 2013 *JHEP* **1301** 063 (*Preprint* 1211.4890)
[26] Khachatryan V *et al.* (CMS Collaboration) 2014 (*Preprint* 1406.0113)
[27] Khachatryan V *et al.* (CMS Collaboration) 2015 (*Preprint* 1503.05467)
[28] Aad G *et al.* (ATLAS Collaboration) 2015 (*Preprint* 1503.03243)
[29] Chatrchyan S *et al.* (CMS Collaboration) 2014 (*Preprint* 1404.4619)
[30] Aad G *et al.* (ATLAS Collaboration) 2014 *JHEP* **1404** 031 (*Preprint* 1401.7610)
[31] Chatrchyan S *et al.* (CMS Collaboration) 2013 *JHEP* **1310** 062 (*Preprint* 1305.7389)
[32] Khachatryan V *et al.* (CMS Collaboration) 2015 *Eur.Phys.J.* **C75** 66 (*Preprint* 1410.3153)
[33] Aad G *et al.* (ATLAS Collaboration) 2014 *Phys.Rev.Lett.* **113** 141803 (*Preprint* 1405.6241)
[34] Chatrchyan S *et al.* (CMS Collaboration) 2013 *JHEP* **1307** 116 (*Preprint* 1305.5596)
[35] Khachatryan V *et al.* (CMS Collaboration) 2015 *Phys.Rev.Lett.* **114** 051801 (*Preprint* 1410.6315)
[36] Aad G *et al.* (ATLAS Collaboration) 2015 (*Preprint* 1503.03709)
[37] Chatrchyan S *et al.* (CMS Collaboration) 2011 *Phys.Rev.* **D84** 112002 (*Preprint* 1110.2682)
[38] Chatrchyan S *et al.* (CMS Collaboration) 2013 *Phys.Lett.* **B718** 752–772 (*Preprint* 1207.3973)
[39] Aad G *et al.* (ATLAS Collaboration) 2008 *JINST* **3** S08003
[40] Abulencia A *et al.* (CDF Collaboration) 2007 *J.Phys.* **G34** 2457–2544 (*Preprint* hep-ex/0508029)
[41] Chatrchyan S *et al.* (CMS Collaboration) 2008 *JINST* **3** S08004
[42] Abazov V *et al.* (D0 Collaboration) 2006 *Nucl.Instrum.Meth.* **A565** 463–537 (*Preprint* physics/0507191)

[43] Alves A Augusto J *et al.* (LHCb Collaboration) 2008 *JINST* **3** S08005
[44] Aaltonen T A *et al.* (CDF Collaboration) 2014 *Phys.Rev.* **D89** 072005 (*Preprint* 1402.2239)
[45] Aaltonen T *et al.* (CDF Collaboration) 2013 *Phys.Rev.* **D88** 072002 (*Preprint* 1307.0770)
[46] Aaltonen T A *et al.* (CDF Collaboration) 2014 *Phys.Rev.* **D89** 072003 (*Preprint* 1311.0894)
[47] Aaltonen T *et al.* (CDF Collaboration) 2012 *Phys.Rev.Lett.* **108** 151803 (*Preprint* 1203.0275)
[48] Abazov V M *et al.* (D0 Collaboration) 2014 *Phys.Rev.Lett.* **112** 151803 (*Preprint* 1312.2895)
[49] Abazov V M *et al.* (D0 Collaboration) 2013 *Phys.Rev.* **D88** 091102 (*Preprint* 1309.2591)
[50] Abazov V M *et al.* (D0 Collaboration) 2014 *Phys.Rev.* **D89** 012005 (*Preprint* 1310.8628)
[51] Abazov V M *et al.* (D0 Collaboration) 2012 *Phys.Rev.Lett.* **108** 151804 (*Preprint* 1203.0293)
[52] Aaltonen T A *et al.* (CDF Collaboration, D0 Collaboration) 2013 *Phys.Rev.* **D88** 052018 (*Preprint* 1307.7627)
[53] Baak M, Blondel A, Bodek A, Caputo R, Corbett T *et al.* 2013 (*Preprint* 1310.6708)
[54] Bozzi G, Rojo J and Vicini A 2011 *Phys.Rev.* **D83** 113008 (*Preprint* 1104.2056)